CellPress

Cell Host & Microbe
Article

Induction of INKIT by Viral Infection Negatively Regulates Antiviral Responses through Inhibiting Phosphorylation of p65 and IRF3

Bin Lu,[1,7] Yujie Ren,[1,7] Xueqin Sun,[1,7] Cuijuan Han,[1] Hongyan Wang,[1] Yuxuan Chen,[1] Qianqian Peng,[5] Yongbo Cheng,[6] Xiaoliang Cheng,[6] Qiyun Zhu,[5] Wenxin Li,[1] Hong-Liang Li,[2,3,4] Hai-Ning Du,[1] Bo Zhong,[1,2,8,*] and Zan Huang[1,*]

[1]Hubei Key Laboratory of Cell Homeostasis, College of Life Sciences, Wuhan University, Wuhan 430072, China
[2]Medical Research Institute
[3]Institute of Model Animals
[4]School of Basic Medical Sciences
School of Medicine, Wuhan University, Wuhan 430071, China
[5]State Key Laboratory of Veterinary Etiological Biology, Lanzhou Veterinary Research Institute, Chinese Academy of Agricultural Sciences, Lanzhou 730046, China
[6]Wuhan Qlife Lab Co., Ltd, Wuhan 430074, China
[7]These authors contributed equally
[8]Lead Contact
*Correspondence: zhongbo@whu.edu.cn (B.Z.), z-huang@whu.edu.cn (Z.H.)
http://dx.doi.org/10.1016/j.chom.2017.06.013

SUMMARY

The transcription factors p65 and IRF3 play key roles in the induction of cellular antiviral responses. Phosphorylation of p65 and IRF3 is required for their activity and constitutes a key checkpoint. Here we report that viral infection induced upregulation of INKIT, an inhibitor for NF-κB and IRF3 that restricted innate antiviral responses by blocking phosphorylation of p65 and IRF3. INKIT overexpression inhibited virus-induced phosphorylation of p65 and IRF3 and expression of downstream genes. In contrast, knockdown or knockout of INKIT had the opposite effect: *Inkit*$^{-/-}$ mice produced elevated levels of type I interferons and proinflammatory cytokines and were more resistant to lethal viral infection compared to wild-type. INKIT interacted with IKKα/β and TBK1/IKKε, impairing the recruitment and phosphorylation of p65 and IRF3. Viral infection induced IKK-mediated phosphorylation of INKIT at Ser58, resulting in its dissociation from the IKKs. Our findings thus uncover INKIT as a regulator of innate antiviral responses.

INTRODUCTION

Viral infection triggers a series of signaling cascades that induce expression of type I interferons (IFNs) and proinflammatory cytokines. Detection of invading viruses by innate immune system depends on pattern recognition receptor (PRR)-mediated recognition of viral nucleic acids (Takeuchi and Akira, 2010). To date, it has been demonstrated that TLR3, TLR7/8, and RIG-I and MDA5 (known as RIG-I-like receptors, or RLRs) detect viral RNA, whereas TLR9 and a number of cytosolic DNA sensors such as cyclic GMP-AMP synthase (cGAS) have been identified to recognize viral DNA in a ligand- and/or cell-type-specific-dependent manner (Pandey et al., 2014; Wu and Chen, 2014). Upon binding of viral nucleic acids, these PRRs recruit downstream adaptor proteins including TRIF (Yamamoto et al., 2003), MyD88 (Wesche et al., 1997), VISA (also called MAVS, Cardif, and IPS-1) (Kawai et al., 2005; Seth et al., 2005; Xu et al., 2005), and MITA (also called STING) (Ishikawa and Barber, 2008; Zhong et al., 2008), which further activate kinases though various mechanisms. For example, the canonical inhibitor of κB kinases (IKKs) consist of two catalytic subunits, IKKα and IKKβ, and a regulatory subunit, IKKγ (also known as NEMO), and IKKα and IKKβ are phosphorylated and activated either by an upstream kinase (such as TAK1) or by trans-autophosphorylation in a higher-order IKKα/β/γ complex (Hayden and Ghosh, 2012; Zhang et al., 2017). The noncanonical IKKs include TBK1 and IKKε, and the activation of TBK1 requires multiple E3 ligase-mediated ubiquitination and GSK3β-mediated trans-autophosphorylation (Lei et al., 2010; Li et al., 2011; Song et al., 2016; Wang et al., 2009).

Nuclear factor kappa B (NF-κB) and interferon-regulated factors (IRFs) are two families of transcription factors that are critically involved in viral infection-induced transcription of downstream genes and activated by the canonical and noncanonical IKKs, respectively (Hinz and Scheidereit, 2014; McWhirter et al., 2004). IRF3 belongs to the IRF family and is essential for the initial expression wave of antiviral genes such as *IFNA*, *IFNB*, *CCL5*, and *ISG15* (Ikushima et al., 2013). Activation of IRF3 depends on phosphorylation of a series of serine residues between aa 380 and aa 427 that is directly mediated by two kinases, TBK1 and IKKε. Gene deletion studies demonstrate that TBK1 and IKKε (to a lesser extent) function redundantly in phosphorylation of IRF3 in various types of cells (Hemmi et al., 2004; Perry et al., 2004). Although it has been reported that SIKE sequesters TBK1 and IKKε from IRF3 in uninfected cells and thereby keeps phosphorylation and activation of IRF3 in check (Huang et al., 2005), it remains largely unknown whether and

how other molecules regulate IRF3 phosphorylation by TBK and IKKε after viral infection.

The NF-κB family consists of five members, p50, p52, p65 (Rel A), Rel B, and c-Rel, and forms 15 potential different hetero- or homo-dimers with distinct functions, of which p65/p50 and p52/Rel B are mostly abundant paradigmatic dimers with transcriptional activity (Hayden and Ghosh, 2008). The p52 precursor p100 (NFKB2) constitutively interacts with Rel B and is phosphorylated by IKKα, followed by ubiquitination and partial degradation into p52 upon certain stimulation, resulting in the active p52/Rel B dimer that migrates into nucleus for transcription. The p65/p50 dimer is sequestered in cytoplasm by IκBα, which is phosphorylated by the IKKα/β/γ complex followed by ubiquitination and degradation, thereby releasing free p65/p50 dimer to enter nucleus (Kanarek and Ben-Neriah, 2012; Liu et al., 2012). In addition, IKKα and IKKβ are reported to directly phosphorylate p65 at Ser536, which is essential for the acetylation at Lys310 and the transcriptional activity of p65 (Sakurai et al., 1999; Yang et al., 2003). However, it is less clear how IKK-mediated phosphorylation of p65 is regulated.

We have previously reported that 12-O-tetradecanoylphorbol-13-acetate (TPA) induces upregulation of chromosome 7 open reading frame 41 (C7ORF41), which promotes human megakaryocyte differentiation (Sun et al., 2014). The homolog of human C7ORF41 in *Xenopus laevis*, Maturin, is involved in neurogenesis (Martinez-De Luna et al., 2013). However, the *in vivo* functions of C7ORF41 and whether it regulates cellular antiviral immune responses are totally unknown. In this study, we generated C7ORF41-deficient mice and investigated its role in innate antiviral signaling. Based on the functions of C7ORF41 described below, we designated it as inhibitor for NF-κB and IRF3 (INKIT). We find that knockdown of INKIT in human cell lines or knockout of INKIT in mice results in potentiated phosphorylation of p65 at Ser536 and IRF3 at Ser396, subsequent induction of antiviral genes, and impaired viral replication after viral infection. Consistently, *Inkit*$^{-/-}$ mice produce elevated levels of antiviral cytokines in the sera after viral infection and are more resistant to lethal viral infection compared to the wild-type controls. INKIT is associated with IKKα/β and TBK1/IKKε and inhibits the recruitment and phosphorylation of p65 and IRF3, respectively. IKKα and TBK1 phosphorylate INKIT at Ser58, which results in disassociation of INKIT from IKKα or TBK1 and thereby allows for the subsequent recruitment and phosphorylation of p65 and IRF3. Our findings thus uncover the role of INKIT as a previously uncharacterized regulator of innate immune responses by modulating p65 and IRF3 phosphorylation.

RESULTS

Viral Infection Induces Upregulation of INKIT in a p65-Dependent Manner

Previously, we have demonstrated that TPA treatment induces the expression of INKIT (C7ORF41), which is inhibited by the IKKβ inhibitor SC-514, indicating an NF-κB-dependent upregulation of INKIT (Sun et al., 2014). Because NF-κB is activated in various signaling pathways such as virus-triggered signaling, we examined whether the expression of INKIT was induced by viral infection. The results suggested that the expression of INKIT was upregulated and decreased at the early and late phase of Sendai virus (SeV), vesicular stomatitis virus (VSV), or herpes simplex virus 1 (HSV-1) infection in human THP-1 cells, respectively (Figure 1A). Interestingly, viral infection-triggered upregulation of INKIT was almost completely diminished by the treatment of the IKKβ inhibitor SC-514 or deficiency of p65 (Figures 1B and 1C). In contrast, treatment of the PI3K inhibitor BKM120 or deficiency of IRF3 and IRF7 had minimal effects on virus-triggered induction of INKIT (Figures 1B and 1D). In parallel experiments, we found that TNFα also induced upregulation of INKIT, which was abrogated by p65 deficiency (Figure S1A). Cell fractionation analysis suggested that INKIT was located in the cytosol in the presence or absence of viral infection (Figure S1B). We have observed that overexpression of p65 strongly induces the activity of *INKIT* promoter, and TPA-induced *INKIT* promoter activity is severely inhibited by SC-514 (Sun et al., 2014). Sequence analysis suggested that there are one or two p65 binding sites on human *INKIT* or mouse *Inkit* promoters, respectively. Results from chromatin immunoprecipitation (ChIP) assays showed that SeV or HSV-1 infection induced p65 binding to the *INKIT* or *Inkit* promoters in both THP-1 cells and primary mouse embryonic fibroblasts (MEFs) (Figure 1E). These data together suggest that viral infection induces upregulation of INKIT in a p65-dependent manner.

INKIT Negatively Regulates Innate Antiviral Signaling

We next examined the role of INKIT in virus-triggered signaling and found that overexpression of INKIT inhibited SeV-induced activation of ISRE, NF-κB, and IFN-β promoter in a dose-dependent manner in reporter assays (Figure 2A). Overexpression of INKIT inhibited SeV- or HSV-1-induced expression of *IFNB1* and *TNFA* in THP-1 cells (Figure 2B). In addition, SeV-induced phosphorylation of p65 (Ser536) and IRF3 (Ser396), but not IκBα, IKKα/β, TBK1, or JNK, was substantially impaired by overexpression of INKIT (Figure 2C), indicating INKIT as a negative regulator of virus-triggered signaling. We made two short hairpin RNA (shRNA) constructs targeting INKIT, both of which inhibited the expression of INKIT in HeLa cells (Figure 2D). Interestingly, knockdown of INKIT by shRNA significantly potentiated the transcription of *IFNB1*, *TNFA*, *ISG56*, and *ISG15* and increased the induction of IFN-β and TNFα after SeV infection (Figures 2E and 2F). Consistent with these observations, knockdown of INKIT substantially potentiated the phosphorylation of p65(Ser536) and IRF3 (Ser396), but not IκBα, IKKα/β, TBK1, or JNK, after SeV infection (Figure 2G). We next examined the effects of INKIT on viral replication and found that overexpression and knockdown of INKIT strongly promoted and inhibited VSV-GFP replication as monitored by the GFP intensities, respectively (Figures 2H and 2I). These data collectively suggest that INKIT negatively regulates virus-triggered phosphorylation of p65 and IRF3 as well as cellular antiviral responses.

INKIT Deficiency Promotes Virus-Triggered Signaling

To examine the function of INKIT in antiviral responses *in vivo*, we generated INKIT-deficient mice by CRISPR/Cas9-mediated genome editing. Sequencing of the mouse *Inkit* genome indicated that there is a 29 bp deletion in the edited allele, which resulted in a frameshift proximal to the start codon of *INKIT* gene (Figures S2A and S2B). Results from immunoblot analysis indicated a complete loss of INKIT expression in mouse bone

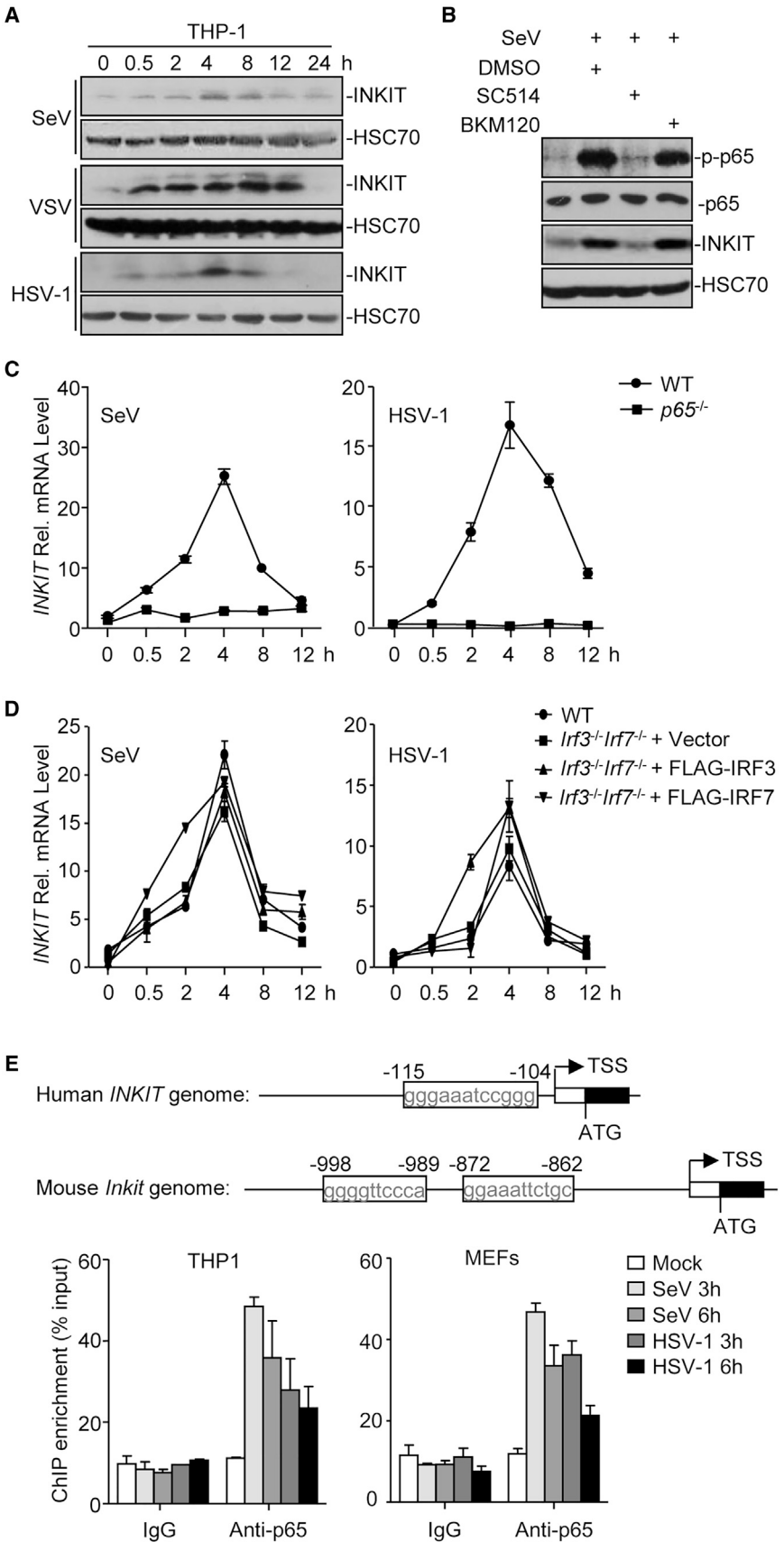

Figure 1. Viral Infection Induces Upregulation of INKIT in a p65-Dependent Manner

(A) Immunoblot analysis (with anti-INKIT and anti-HSC70) of THP-1 cells infected with SeV, VSV, or HSV-1 for 0–24 hr.

(B) Immunoblot analysis (with anti-p-p65, anti-p65, anti-INKIT, and anti-HSC70) of THP-1 cells pretreated with DMSO, SC-514, or BKM-120 for 1 hr followed by infection with or without SeV for 4 hr.

(C) qRT-PCR analysis of *INKIT* mRNA in wild-type and p65 knockout ($p65^{-/-}$) MEFs infected with SeV or HSV-1 for 0–8 hr.

(D) qRT-PCR analysis of *INKIT* mRNA in wild-type MEFs, $Irf3^{-/-}Irf7^{-/-}$ MEFs reconstituted with empty vector, IRF3, or IRF7 followed by infection with SeV or HSV-1 for 0–8 hr.

(E) Analysis of human and mouse *INKIT* genome (upper) and ChIP analysis of p65 binding on the promoter of *INKIT* gene in THP-1 cells (lower left) and MEFs (lower right).

Data are representative of three independent experiments (mean ± SD in C–E, n = 3). See also Figure S1.

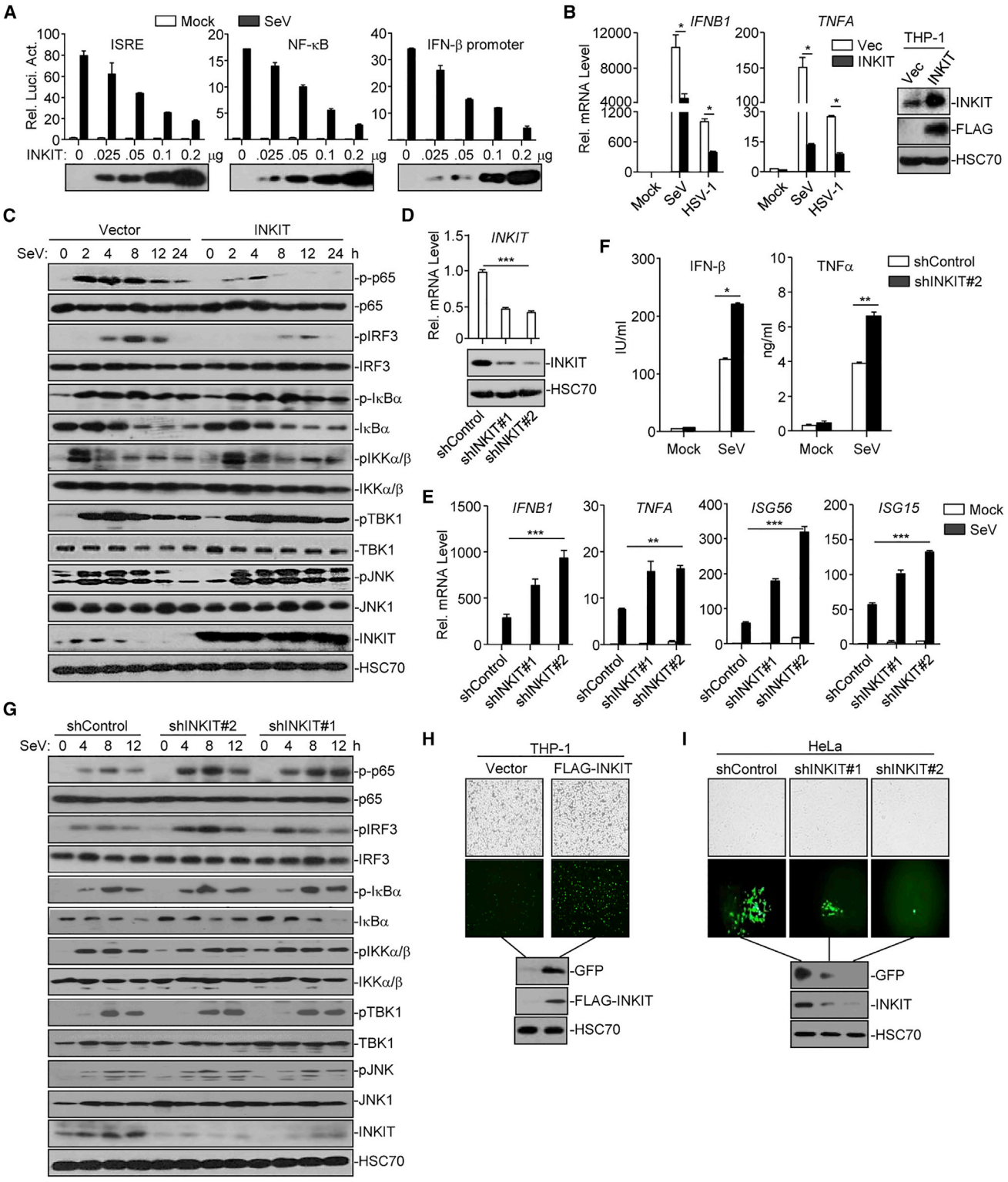

Figure 2. INKIT Negatively Regulates Innate Antiviral Signaling

(A) Luciferase reporter assays analyzing ISRE, NF-κB, and IFN-β promoter activity (upper graphs) and immunoblot assay with anti-FLAG (lower panels) of HEK293 cells transfected with empty vector or plasmids encoding FLAG-INKIT (0.025–0.2 μg) for 20 hr followed by infection with SeV for 8 hr.

(B) qRT-PCR analysis (left graphs) of *IFNB* and *TNFA* mRNA and immunoblot analysis (with anti-INKIT, anti-FLAG, or anti-HSC70) (right panels) of THP-1 cells stably transfected with empty vector or plasmid encoding INKIT followed by infection with SeV or HSV-1 for 8 hr.

(legend continued on next page)

marrow cells (Figure S2C). The *Inkit*$^{-/-}$ mice were born at the Mendelian ratio and did not display any developmental abnormality, suggesting that INKIT is dispensable for the growth and development of mice. The number and composition of cells of the immune response in various organs (including thymus, spleen, and peripheral lymph nodes) were similar in 2- to 3-month-old *Inkit*$^{-/-}$ mice and their wild-type littermates (Figures S2D–S2F), indicating that INKIT is not required for the development of various types of cells of the immune response.

We next examined the effects of INKIT deficiency on virus-triggered expression of downstream genes. Results of qRT-PCR analysis showed that the expression of *Ifnb*, *Ifna4*, *Ifnan*, *Il6*, and *Tnf* was significantly increased in *Inkit*$^{-/-}$ bone marrow-derived dendritic cells (BMDCs), bone marrow-derived macrophages (BMDMs), or MEFs compared to the wild-type counterparts after SeV, VSV, or HSV-1 infection, or transfection of poly(I:C) or various DNA ligands (Figures 3A, S3A, and S3B). The production of IFN-β, IL-6, or TNFα by *Inkit*$^{-/-}$ BMDCs, BMDMs, or MEFs was significantly higher than that by the wild-type counterparts after SeV, VSV, or HSV-1 infection or transfection of poly(I:C) or DNA ligands (Figures 3B and S3C). Consistent with the results from gene induction and ELISA assays, the phosphorylation of p65 (Ser536) and IRF3 (Ser396), but not IκBα, IKKα/β, TBK1, or ERK, substantially increased in *Inkit*$^{-/-}$ BMDCs compared to wild-type BMDCs after SeV, HSV-1, or VSV infection (Figures 3C and S3D). Collectively, these results suggest that INKIT negatively regulates virus-triggered induction of downstream genes by inhibiting phosphorylation of p65 and IRF3.

We next analyzed the effects of INKIT deficiency on viral replication. Results of qRT-PCR and plaque assays suggested that the expression of HSV-1 *UL30* gene and the replication of HSV-1 were significantly inhibited in *Inkit*$^{-/-}$ MEFs compared to the wild-type MEFs (Figure 3D). In addition, the replication of HSV-1-GFP or VSV-GFP was more severely compromised in *Inkit*$^{-/-}$ MEFs than in *Inkit*$^{+/+}$ MEFs as monitored by the GFP percentages and intensities (Figures 3E and S3E). Taken together, these data suggest that INKIT restricts viral infection-induced activation of p65 and IRF3 and thereby promotes viral replication.

INKIT-Deficient Mice Exhibit Resitance to Lethal VSV or HSV-1 Infection

To examine the physiological role of INKIT in host defense against viral infection, we infected the *Inkit*$^{-/-}$ mice and wild-type littermates by intravenous injection of HSV-1 and monitored the survival of mice. All the wild-type mice exhibited severe lethargy and ataxia at day 5 after infection and died quickly after the appearance of the symptoms. In contrast, one out of five *Inkit*$^{-/-}$ mice displayed such symptoms and died on day 7 after infection (Figure 4A). Consistently, the levels of IFN-β, IL-6, and CXCL1 in the sera and the expression of *Ifnb*, *Ifna4*, *Il6*, *Cxcl1*, and *Ccl5* in the lungs were significantly increased in the *Inkit*$^{-/-}$ mice compared to those in *Inkit*$^{+/+}$ littermates 12 or 24 hr after HSV-1 infection, respectively (Figures 4B and 4C). To evaluate the importance of INKIT for viral replication *in vivo*, we intranasally injected HSV-1 into the *Inkit*$^{-/-}$ mice and wild-type littermates and 4 days later the expression of antiviral genes and HSV-1 titers in the brains were analyzed. The results showed that the mRNA levels of *Ifnb*, *Ifna4*, and *Ccl5* were significantly higher in the brains of *Inkit*$^{-/-}$ mice than in the brains of *Inkit*$^{+/+}$ littermates, whereas the mRNA levels of HSV-1 *UL30* gene and the HSV-1 viral titers were significantly decreased in the brains of *Inkit*$^{-/-}$ mice compared to the brains of *Inkit*$^{+/+}$ littermates (Figures 4D and 4E), indicating that INKIT restricts antiviral responses against HSV-1 *in vivo*.

We next infected the *Inkit*$^{-/-}$ mice and wild-type littermates by intravenous injection of VSV and monitored their survival. As shown in Figure 4F, the wild-type mice began to die on day 9 and all of them died on day 11 after infection. In contrast, *Inkit*$^{-/-}$ mice began to die on day 10 and 60% (3 out of 5) of *Inkit*$^{-/-}$ mice finally survived from weak ataxia and paralysis. Consistent with these observations, the protein levels of IFN-β, IL-6, and TNFα in the sera of *Inkit*$^{-/-}$ mice and the mRNA levels of *Ifnb*, *Ifna4*, *Il6*, *Tnf*, and *Cxcl1* in the lungs of *Inkit*$^{-/-}$ mice were significantly higher than in those of *Inkit*$^{+/+}$ mice at 12 or 24 hr after VSV infection, respectively (Figures 4G and 4H). In addition, the replication of VSV in the lungs of *Inkit*$^{-/-}$ mice was severely compromised compared to the *Inkit*$^{+/+}$ littermates (Figure 4I). These data collectively suggest that INKIT negatively regulates innate immune responses against viruses by inhibiting the production of type I IFNs and proinflammatory cytokines.

INKIT Interacts with IKKs and TBK1 and Functions at IRF3 and p65 Level

To understand the mechanisms by which INKIT regulates innate antiviral signaling, we examined the level of INKIT involved in the molecular order of PRR-triggered signaling by luciferase reporter

(C) Immunoblot analysis of phosphorylated and total p65, IRF3, IκBα, IKKα/β, TBK1 or JNK, total INKIT, and β-actin of THP-1 cells stably transfected with empty vector or plasmid encoding FLAG-INKIT followed by infection with SeV for 0–24 hr.

(D) qRT-PCR analysis (upper graph) of INKIT mRNA and immunoblot analysis (with anti-INKIT and anti-HSC70) (lower panels) of HeLa cells stably transfected with an empty shRNA vector (shControl), or shRNA targeting INKIT (shINKIT#1 or shINKIT#2).

(E) qRT-PCR analysis of *IFNB*, *TNFA*, *ISG65*, and *ISG15* mRNA of HeLa cells stably transfected with shControl, shINKIT#1, or shINKIT#2 followed by infection with SeV for 8 hr.

(F) ELISA analysis of IFN-β and TNFα in the supernatants of HeLa cells stably transfected with plasmids encoding shControl or shINKIT#2 followed by infection with SeV for 24 hr.

(G) Immunoblot analysis of phosphorylated and total p65, IRF3, IκBα, IKKα/β, TBK1 or JNK, total INKIT, and β-actin of HeLa cells stably transfected with shControl, shINKIT#1, or shINKIT#2 followed by infection with SeV for 0–12 hr.

(H) Fluorescent microscopy imaging (upper) and immunoblot analysis (with anti-GFP, anti-FLAG, and anti-HSC70) (lower panels) of THP-1 cells stably transfected with empty vector or plasmids encoding FLAG-INKIT for 24 hr followed by infection with VSV-GFP for 24 hr.

(I) Fluorescent microscopy imaging (upper) and immunoblot analysis (with anti-GFP, anti-INKIT, and anti-HSC70) (lower panels) of HeLa cells stably transfected with shControl, shINKIT#1, or shINKIT#2 followed by infection with VSV-GFP for 24 hr.

*$p < 0.05$; **$p < 0.01$; ***$p < 0.001$ (two-way ANOVA followed by Bonferroni post-test). Data are representative of three independent experiments (mean ± SD in A, B, and D–F, n = 3).

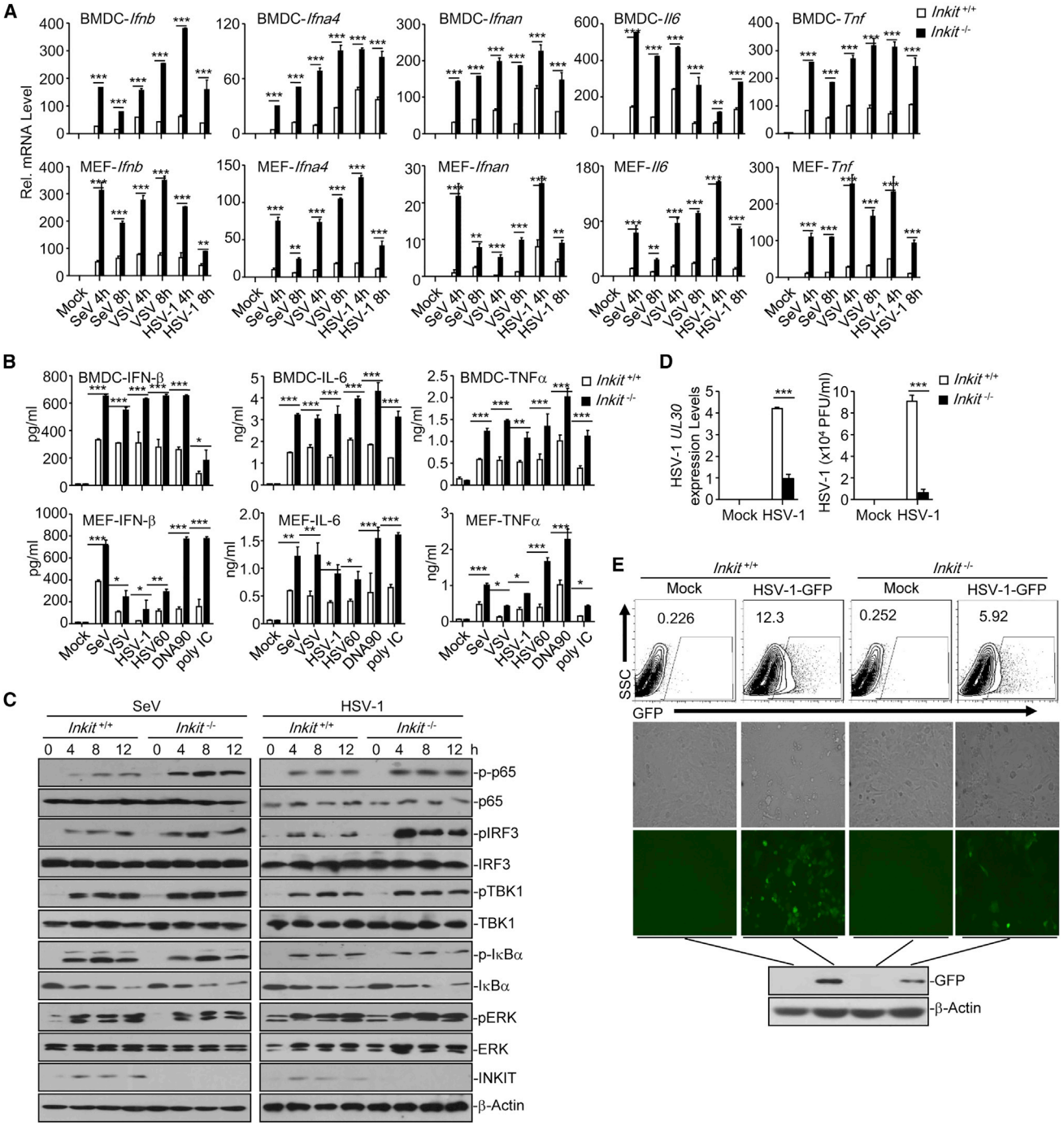

Figure 3. INKIT Deficiency Promotes Virus-Triggered Signaling

(A) qRT-PCR analysis of *Ifnb*, *Ifna4*, *Ifnan*, *Il6*, and *Tnf* mRNA in *Inkit*$^{+/+}$ and *Inkit*$^{-/-}$ BMDCs (upper graphs) or MEFs (lower graphs) infected with SeV, VSV, or HSV-1 for 0–8 hr.

(B) ELISA analysis of IFN-β, IL-6, and TNFα in the supernatants of *Inkit*$^{+/+}$ and *Inkit*$^{-/-}$ BMDCs (upper graphs) or MEFs (lower graphs) infected with SeV, VSV, or HSV-1 for 24 hr or mock transfected (Lipo) or transfected with HSV60, DNA90, or poly IC for 12 hr.

(C) Immunoblot analysis of phosphorylated and total p65, IRF3, TBK1, IκBα or ERK, total INKIT, and β-actin in *Inkit*$^{+/+}$ and *Inkit*$^{-/-}$ BMDCs infected with SeV (left) or HSV-1 (right) for 0–12 hr.

(D) *Inkit*$^{+/+}$ and *Inkit*$^{-/-}$ MEFs (5×10^5) left uninfected or infected with HSV-1 (MOI = 0.1) for 1 hr, after which they were washed twice in PBS and cultured in full medium for 24 hr. Cells and the supernatants were harvested for qRT-PCR analysis of HSV-1 *UL30* mRNA (left) or plaque assays (right), respectively.

(legend continued on next page)

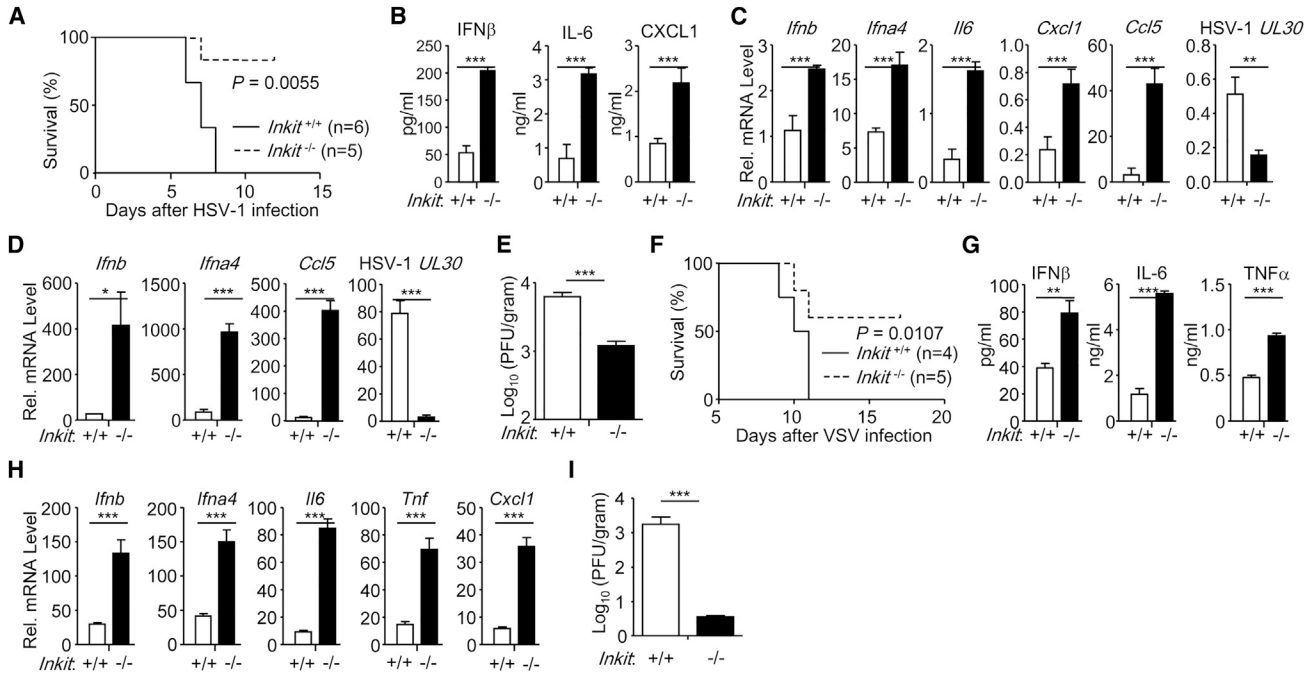

Figure 4. INKIT-Deficient Mice Are More Resistant to Lethal VSV or HSV-1 Infection

(A) Survival (Kaplan-Meier curve) of *Inkit*$^{+/+}$ (n = 6) and *Inkit*$^{-/-}$ mice (n = 5) intravenously injected with HSV-1 (2.5 × 10^6 PFU [plaque-forming unit] per mouse) monitored for 12 days.

(B and C) ELISA analysis of IFN-β, IL-6, and CXCL1 in the sera (B) or qRT-PCR analysis of *Ifnb*, *Ifna4*, *Il6*, *Cxcl1*, *Ccl5*, or HSV-1 *UL30* mRNA in the lungs (C) of *Inkit*$^{+/+}$ and *Inkit*$^{-/-}$ mice (n = 4) intravenously injected with HSV-1 (1 × 10^6 PFU/mouse) for 12 or 24 hr.

(D and E) qRT-PCR analysis of *Ifnb*, *Ifna4*, *Ccl5*, or HSV-1 *UL30* mRNA in the brains (D) and plaque assays of the brain homogenizes (E) from *Inkit*$^{+/+}$ and *Inkit*$^{-/-}$ mice intranasally injected with HSV-1 (2.5 × 10^6) for 4 days.

(F) Survival (Kaplan-Meier curve) of *Inkit*$^{+/+}$ (n = 4) and *Inkit*$^{-/-}$ mice (n = 5) intravenously injected with VSV (2 × 10^7 PFU per mouse) monitored for 18 days.

(G and H) ELISA analysis of IFN-β, IL-6, and TNFα in the sera (G) and qRT-PCR analysis of *Ifnb*, *Ifna4*, *Il6*, *Tnf*, or *Cxcl1* mRNA in the lungs (H) from *Inkit*$^{+/+}$ and *Inkit*$^{-/-}$ mice (n = 3) intravenously injected with VSV (1 × 10^7 PFU per mouse) for 12 or 24 hr.

(I) Plaque assays of the lungs from *Inkit*$^{+/+}$ and *Inkit*$^{-/-}$ mice (n = 4) intravenously injected with VSV (1 × 10^7 PFU per mouse) for 4 days.

*p < 0.05; **p < 0.01; ***p < 0.001 (unpaired Student's t test). Data are representative of three independent experiments (mean ± SD in B–E and G–I).

assays. The results showed that overexpression of INKIT inhibited activation of NF-κB mediated by p65 and its upstream molecules (including RIG-I, VISA, TRAF6, IKKα, and IKKβ), as well as activation of ISRE mediated by IRF3 and its upstream molecules (including RIG-I, MITA, VISA, TBK1, and IKKε) (Figure 5A), whereas knockdown of INKIT had opposite effects (Figure 5B). Interestingly, IRF3-5D (a constitutively active form of IRF3)-mediated activation of ISRE was not affected by either overexpression or knockdown of INKIT. Results from transient transfection and co-immunoprecipitation assays suggested that INKIT interacted with IKKα, IKKβ, TBK1, and IKKε, but not with IKKγ, VISA, or MITA (Figure S4). Endogenous immunoprecipitation analysis suggested that INKIT constitutively interacted with IKKα/β and SeV infection or transfection of poly(I:C) led to INKIT dissociation from IKKα/β at later time points (Figure 5C). In contrast, INKIT interacted with TBK1 or IKKε at the early time point after SeV infection and the associations were impaired at the late time point after SeV infection or transfection of poly(I:C) (Figure 5C). Domain mapping analysis suggests that the N-terminal kinase domain of IKKα, TBK1, or IKKε was responsible for their association with INKIT (Figure 5D). These data together suggest that INKIT interacts with the canonical and noncanonical IKKs and functions at the level of p65 and IRF3.

INKIT Impairs the Recruitment of p65 and IRF3 to the IKKs and TBK1

Because INKIT interacts with the canonical and noncanonical IKKs and functions at the level of p65 and IRF3, we reasoned that INKIT might interfere with the interaction between p65 and IKKα/β or the interaction between IRF3 and TBK1/IKKε. Results from transient transfection and co-immunoprecipitation assays suggested that the interactions between TBK1 or IKKε and IRF3 and between IKKα or IKKβ and p65 were substantially impaired by INKIT (Figures 6A and 6B). In contrast, the interactions between IKKβ and IKKα or IκBα and the TBK1-TBK1 or

(E) Flow cytometry analysis (upper), fluorescent microscopy imaging (middle), and immunoblot analysis with anti-GFP and anti-β-actin (bottom) of *Inkit*$^{+/+}$ and *Inkit*$^{-/-}$ MEFs infected with or without HSV-1-GFP for 24 hr.

*p < 0.05; **p < 0.01; ***p < 0.001 (two-way ANOVA followed by Bonferroni post-test). Data are representative of three independent experiments (mean ± SD in A, B, and D, n = 3). See also Figures S2 and S3.

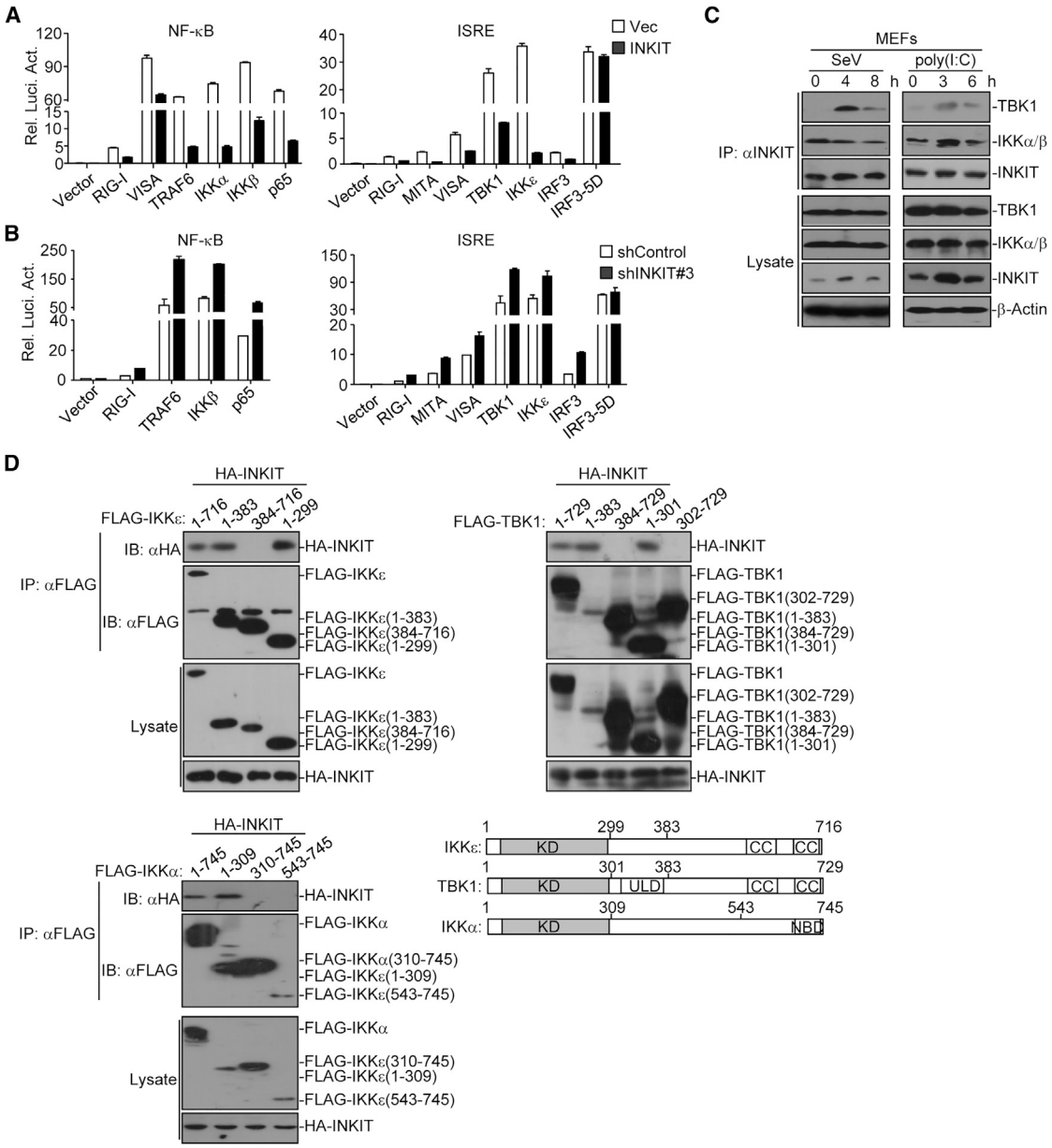

Figure 5. INKIT Functions at IRF3 and p65 Level

(A) Luciferase reporter assays analyzing NF-κB and ISRE activity of HEK293 cells transfected with empty vector or plasmids encoding RIG-I, VISA, TRAF6, IKKα, IKKβ, p65, MITA, TBK1, IKKε, IRF3, or IRF3-5D together with an empty vector or INKIT for 24 hr.

(B) Luciferase reporter assays analyzing NF-κB and ISRE activity of HEK293 cells transfected with empty vector or plasmids encoding RIG-I, VISA, TRAF6, IKKα, IKKβ, p65, MITA, TBK1, IKKε, IRF3, and IRF3-5D together with plasmids shControl or shINKIT#2 for 24 hr.

(C) Immunoprecipitation analysis (with anti-INKIT) and immunoblot analysis (with anti-TBK1, anti-IKKα/β, anti-INKIT, or anti-β-actin) of MEFs infected with SeV (left graph) or transfected with poly(I:C) (4 μg) (right graph) for 0–8 or 0–6 hr, respectively.

(D) Immunoprecipitation analysis (with anti-FLAG) and immunoblot analysis (with anti-FLAG or anti-HA) of HEK293 cells transfected with plasmids encoding HA-INKIT and FLAG-tagged TBK1, FLAG-IKKε, IKKα, or their truncations for 24 hr.

KD, kinase domain; ULD, ubiquitin-like domain; CC, coiled-coil domain; NBD, NEMO-binding domain. Data are representative of three (A and B) or two (C and D) independent experiments (mean ± SD in A and B, n = 3). See also Figure S4.

TBK1-adaptor protein (VISA, MITA, or TRIF) associations were not affected by INKIT (Figure S5). In addition, we found that SeV-induced IKKα/β-p65 or TBK1/IKKε-IRF3 associations were more substantially potentiated in *Inkit*$^{-/-}$ BMDCs than in wild-type BMDCs (Figure 6C). Collectively, these data suggest that INKIT inhibits the recruitment of p65 and IRF3 to and thereby impairs the phosphorylation and activation of p65 and IRF3 by the canonical and noncanonical IKKs, respectively.

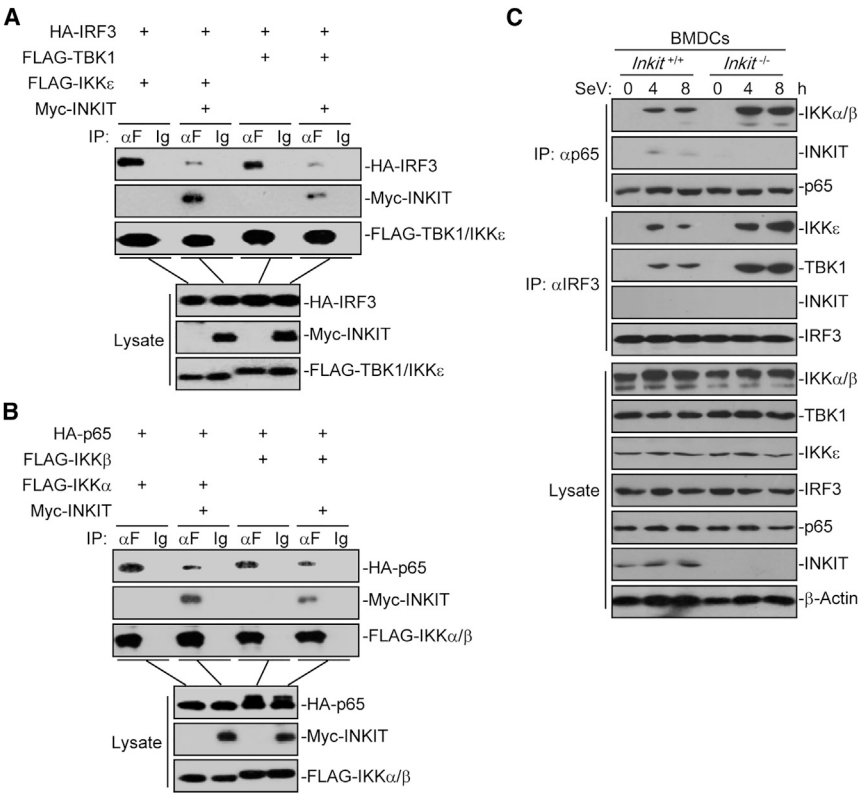

Figure 6. INKIT Impairs the Recruitment of p65 and IRF3 to the IKKs and TBK1

(A and B) Immunoprecipitation analysis (with anti-FLAG or IgG as a control) and immunoblot analysis (with anti-HA, anti-Myc, or anti-FLAG) of HEK293 cells transfected with plasmids encoding HA-IRF3 and Myc-INKIT or empty vector together with FLAG-TBK1 or FLAG-IKKε (A) or transfected with plasmids encoding HA-p65 and Myc-INKIT or vector together with FLAG-IKKα or FLAG-IKKβ (B) for 24 hr.

(C) Immunoprecipitation analysis (with anti-IRF3 or anti-p65) and immunoblot analysis (with anti-INKIT, anti-β-actin and anti-IKKα/β, anti-p65 or anti-IKKε, anti-TBK1, anti-IRF3, or anti-β-actin) of MEFs infected with SeV for 0–8 hr.

Data are representative of three independent experiments. See also Figure S5.

Ser58 of INKIT Is Critical for Suppression of p65 and IRF3 Activation

Because INKIT interacted with the canonical and noncanonical IKKs, which are serine/threonine kinases, we hypothesized that INKIT might be phosphorylated on the serine or threonine residues upon viral infection. Immunoblot analysis indicated that INKIT was phosphorylated on serine residues at the early phase of SeV infection, which was diminished at the late phase of SeV infection (Figure S6A). Overexpression of IKKα and TBK1 strongly induced serine phosphorylation of INKIT in the presence or absence of SeV infection (Figure S6B). Treatment of the IKKα/β inhibitor (IMD0354) or the TBK1/IKKε inhibitor (ZM449829), but not the p38 MAPK inhibitor, substantially impaired SeV-induced serine phosphorylation of INKIT (Figure S6C). In addition, SeV-induced serine phosphorylation of INKIT was substantially impaired in *Tbk1*$^{-/-}$ MEFs transfected with siIKKε and treated with IKKα/β inhibitors (Figure S6D), indicating that the canonical and noncanonical IKKs mediate phosphorylation of INKIT on the serine residues after viral infection.

We next made a series of INKIT mutants in which the conserved serine residues were individually mutated into either alanine (A) or aspartic acid (D) residues and examined their ability to suppress SeV-triggered activation of IFN-β promoter. Interestingly, mutation of Ser58 of INKIT into Asp failed to inhibit SeV-induced activation of IFN-β promoter and potentiated IKKα-mediated phosphorylation of INKIT *in vitro*, whereas mutation of Ser58 of INKIT into Ala inhibited SeV-induced activation of IFN-β promoter and severely impaired SeV- or transfected poly(I:C)-induced or IKKα-mediated phosphorylation of INKIT (Figures 7A, 7B, S6E, and S6F). INKIT(S58D) neither inhibited SeV-induced phosphorylation of p65 and IRF3 nor potentiated VSV-GFP replication as did wild-type INKIT (Figures S7A and S7B), indicating that phosphorylation of Ser58 of INKIT leads to loss of the ability to inhibit virus-triggered signaling. Consistent with this notion, INKIT(S58D) (which mimics phosphorylation on Ser58) substantially lost its ability to interact with IKKα/β or TBK1/IKKε or interfere with IKKα/β-p65 or TBK1/IKKε-IRF3 associations, whereas INKIT(S58A) still interacted with IKKα/β or TBK1/IKKε to interfere with IKKα/β-p65 or TBK1/IKKε-IRF3 associations (Figures 7C, S7C, and S7D), indicating an essential role of Ser58 of INKIT in suppressing innate antiviral signaling.

To further substantiate this conclusion, we reconstituted empty vector, wild-type INKIT, INKIT(S58D), or INKIT(S58A) into *Inkit*$^{-/-}$ MEFs and examined virus-triggered induction of downstream genes. As expected, reconstitution of wild-type INKT or INKIT(S58A), but not INKIT(S58D), inhibited SeV-, VSV-, or HSV-1-induced expression of *Ifnb*, *Ifna4*, *Tnf*, or *Il6* (Figure 7D). Consistently, the phosphorylation of p65 (Ser536) and IRF3 (Ser396) was suppressed in *Inkit*$^{-/-}$ MEFs reconstituted with wild-type INKIT or INKIT(S58A), but not with INKIT(S58D), after SeV, VSV, or HSV-1 infection (Figures 7E and S7E). In addition, VSV-GFP replication was restricted in *Inkit*$^{-/-}$ MEFs reconstituted with INKIT(S58D), but not with wild-type INKIT or INKIT(S58A), as monitored by the GFP percentages (Figure S7F). Consistently, transfected poly(I:C)-induced TBK1-IRF3 or IKKα-p65 associations were impaired in *Inkit*$^{-/-}$ MEFs reconstituted with INKIT or INKIT(S58A), but not with INKIT(S58D) (Figure S7G). These data together suggest that the Ser58 of INKIT is a key site for suppression of p65 and IRF3 activation and cellular antiviral responses.

DISCUSSION

The transcription factors p65 and IRF3 are critically involved in virus-triggered induction of downstream genes and the activation of p65 and IRF3 depends on phosphorylation by the

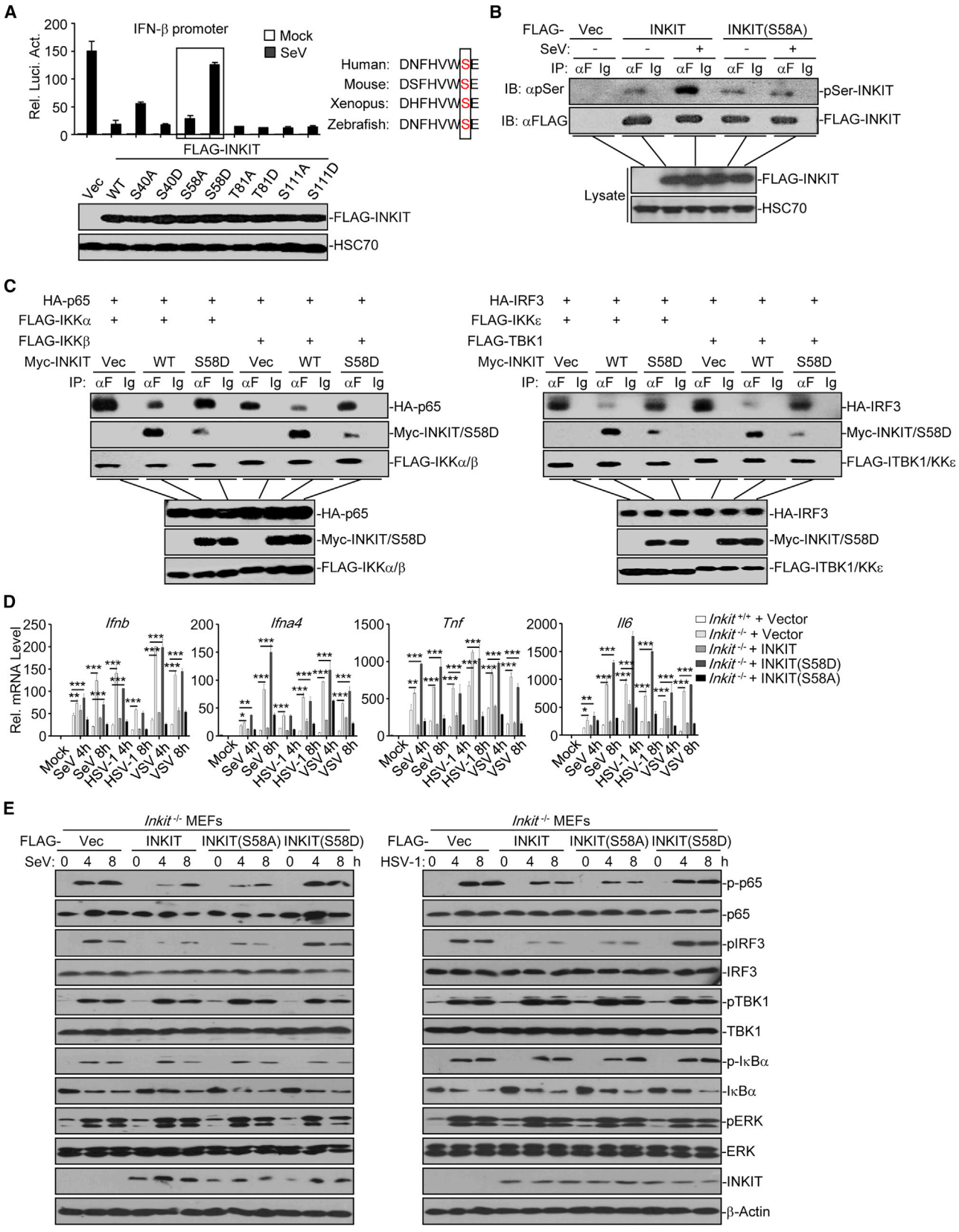

(legend on next page)

canonical and noncanonical IKKs, respectively. In this study, we identified a negative feedback loop of virus-triggered signaling mediated by INKIT (encoded by *C7ORF41*). Viral infection induced p65-dependent expression of INKIT, which subsequently inhibited phosphorylation of p65 and IRF3 as well as cellular antiviral responses by interfering with the association between IKKα/β and p65 and the association between TBK1/IKKε and IRF3. In support of this conclusion, we observed that deficiency or knockdown of INKIT in primary mouse cells or human cell lines resulted in increased IKKα/β-p65 and TBK1/IKKε-IRF3 association, hyperphosphorylation of p65 and IRF3, and increased induction of downstream genes after viral infection. In addition, *Inkit*$^{-/-}$ mice produced elevated type I IFNs and proinflamatory cytokines after viral infection and exhibited resistance to lethal VSV or HSV-1 infection compared to the wild-type littermates. These data together suggest that INKIT is a regulator of host innate antiviral responses.

We have previously reported that INKIT/C7ORF41 is induced by TPA treatment and is involved in megakaryocyte differentiation (Sun et al., 2014). In the present study, we further found that INKIT negatively regulated innate antiviral signaling at the level of p65 and IRF3 phosphorylation. First, overexpression of INKIT or deficiency in INKIT inhibited or potentiated virus-triggered phosphorylation of p65 at Ser536 and IRF3 at Ser396, but not the upstream molecules, including IKKα/β and TBK1, respectively. Second, overexpression or knockdown of INKIT inhibited and potentiated activation of NF-κB or ISRE reporters mediated by p65, IRF3, and their upstream signal transducers, respectively. In contrast, the IRF3-5D (a constitutively active form of IRF3 whose activation does not require phosphorylation by TBK1/IKKε)-mediated activation of ISRE was not affected either by overexpression or by knockdown of INKIT. Third, INKIT specifically interacted with IKKα/β and TBK1/IKKε, but not the upstream adaptors, including VISA and MITA. Thus, unlike SIKE, which suppresses the association between IRF3 and TBK1/IKKε in uninfected cells and restricts IRF3, but not NF-κB activation (Huang et al., 2005), INKIT simultaneously regulated virus-triggered signaling at the level of p65 and IRF3 phosphorylation after viral infection.

Our results suggest that viral infection triggers IKKα/β- and TBK1/IKKε-mediated phosphorylation of INKIT at Ser58. KKα and TBK1 induced phosphorylation on serine residues of INKIT, whereas treatment of IKKα/β and TBK1/IKKε inhibitors or deficiency in TBK1 and IKKε significantly impaired virus-triggered phosphorylation on the serine residues of INKIT. In addition, mutation of Ser58 of INKIT into Ala substantially impaired virus-triggered serine phosphorylation of INKIT in cells or *in vitro*, indicating that Ser58 of INKIT is phosphorylated after viral infection. Interestingly, mutation of Ser58 of INKIT into Asp (which mimics phosphorylation) impaired its ability to interact with IKKα/β or TBK1/IKKε and failed to interfere with the IKKα/β-p65 and TBK1/IKKε-IRF3 associations, indicating that phosphorylation of INKIT by IKKα/β or TBK1/IKKε promotes its disassociation from IKKα/β or TBK1/IKKε. In support of this notion, we found that reconstitution of INKIT(S58D), but not INKIT(S58A), into *Inkit*$^{-/-}$ MEFs failed to inhibit virus-triggered phosphorylation of p65 and IRF3 as well as subsequent induction of downstream genes.

It should be noted that INKIT(S58A) exhibited stronger binding to TBK1/IKKε or IKKα/β than did wild-type INKIT in transient transfection and co-immunoprecipitation assays, whereas GST-INKIT or GST-INKIT(S58A) exhibited comparable binding to TBK1 in GST pull-down assays. A simplest explanation for this is that the amount of INKIT protein used in GST pull-down assays was much more than that in transfected cells. In addition, although GST-INKIT(S58D) weakly interacted with TBK1 or IKKα, it was hyperphosphorylated by IKKα, indicating that Ser58 phosphorylation is a rate-limiting step of TBK1- or IKKα-mediated phosphorylation of INKIT. In addition to viral infection-induced phosphorylation, the serine residues of overexpressed INKIT were basally phosphorylated, which was not affected by viral infection or inhibitors for IKKα/β or TBK1/IKKε in HEK293 cells. However, the basal phosphorylation of INKIT was undetectable in *Tbk1*$^{-/-}$ MEFs stably transfected with TBK1. It is not clear whether the different basal phosphorylation status of INKIT is due to different amounts of basal INKIT proteins or distinct cell types. Further studies are required to elucidate the phosphorylation status of INKIT in unstimulated cells and identify the related kinases for and the physiological relevance of such modifications.

It is interesting to note that the mRNA, protein, and phosphorylation levels of INKIT are upregulated and decreased at the early and late phase of viral infection, respectively. Although the downregulation of INKIT at the late phase of infection is not clear, it possibly involves multiple levels of modulations from transcriptional to posttranslational regulation. Based on our findings and previously published studies, we proposed a model of INKIT-mediated regulation of innate antiviral responses. In resting cells,

Figure 7. Ser58 of INKIT Is Critical for Suppression of p65 and IRF3 Activation

(A) Luciferase reporter assays analyzing IFN-β promoter activity (upper graph) and immunoblot analysis (with anti-FLAG and anti-HSC70) (lower panels) of HEK293 cells transfected with empty vector or plasmids encoding FLAG-INKIT, FLAG-INKIT(S40A), FLAG-INKIT(S40D), FLAG-INKIT(S58A), FLAG-INKIT(S58D), FLAG-INKIT(T81A), FLAG-INKIT(T81D), FLAG-INKIT(S111A), or FLAG-INKIT(S111D) for 24 hr then infected with or without (Mock) SeV for 8 hr.

(B) Immunoprecipitation analysis (with anti-FLAG or IgG as a control) and immunoblot analysis (with anti-pSer, anti-FLAG, and anti-HSC70) of HEK293 cells transfected with empty vector or plasmids encoding FLAG-INKIT or FLAG-INKIT(S58A) then infected with or without (Mock) SeV for 4 hr.

(C) Immunoprecipitation analysis (with anti-FLAG or IgG as a control) and immunoblot analysis (with anti-HA, anti-Myc, and anti-FLAG) of HEK293 cells transfected with HA-p65 and vector, Myc-INKIT, or Myc-INKIT(S58D) together with FLAG-IKKα or FLAG-IKKβ (left) or transfected with HA-IRF3 and vector, Myc-INKIT, or Myc-INKIT(S58D) together with FLAG-TBK1 or FLAG-IKKε (right).

(D) qRT-PCR analysis of *Ifnb*, *Ifna*, *Tnf*, or *Il6* mRNA of *Inkit*$^{+/+}$ MEFs transfected with an empty vector and *Inkit*$^{-/-}$ MEFs reconstituted with an empty vector, INKIT, INKIT (S58A), or INKIT (S58D) followed by infection with SeV, HSV-1, or VSV for 0–8 hr.

(E) Immunoblot analysis of phosphorylation of p65, IRF3, IκBα, TBK1, and ERK or total p65, IRF3, IκBα, TBK1, ERK, INKIT, and β-actin of *Inkit*$^{-/-}$ MEFs reconstituted with empty vector, INKIT, INKIT (S58A), or INKIT (S58D) followed by infection with SeV (left) or HSV-1 (right) for 0–8 hr.

*$p < 0.05$; **$p < 0.01$; ***$p < 0.001$ (two-way ANOVA followed by Bonferroni post-test). Data are representative of three independent experiments (mean ± SD in A and D, n = 3). See also Figures S6 and S7.

a portion of INKIT constitutively interacted with IKKα/β. After viral infection, IKKα/β are activated by phosphorylation, which phosphorylates INKIT at Ser58, leading to the disassociation of INKIT and the recruitment of p65 to IKKα/β. IKKα/β-mediated phosphorylation of p65 at Ser536 results in upregulation of INKIT, which is recruited to TBK1/IKKε to block the recruitment of IRF3. TBK1/IKKε phosphorylates INKIT at Ser58, and this modification leads to its disassociation from TBK1/IKKε, which allows the recruitment and phosphorylation of IRF3. This "hop-on and hop-off " model allows a prompt and proper activation of p65 and IRF3. Our results provide important insights into the molecular mechanisms of the elegant regulation of innate antiviral immune responses.

STAR★METHODS

Detailed methods are provided in the online version of this paper and include the following:

- KEY RESOURCES TABLE
- CONTACT FOR REAGENT AND RESOURCE SHARING
- EXPERIMENTAL MODEL AND SUBJECT DETAILS
  - Mouse Models
  - Cell Lines and Primary Cultures
- METHOD DETAILS
  - Quantitative Real-Time PCR and ELISA
  - Chromatin Immunoprecipitation Assays
  - Reporter Gene Assays
  - Co-immunoprecipitation and Immunoblot Analysis
  - Viral Infection and Plaque Assays
  - Lentivirus-Mediated Gene Transfer
  - Preparation of Nuclear and Cytoplasmic Extractions
  - Protein Purification and GST Pull-Down Assay
  - In Vitro Kinase Assay
- QUANTIFICATION AND STATISTICAL ANALYSIS

SUPPLEMENTAL INFORMATION

Supplemental Information includes seven figures and one table and can be found with this article online at http://dx.doi.org/10.1016/j.chom.2017.06.013.

AUTHOR CONTRIBUTIONS

B.Z. and Z.H. designed and supervised the study; B.L., Y.R., X.S., C.H., H.W., Y. Chen, Q.P., and Y. Cheng performed the experiments and analysis; X.C., Q.Z., W.L., H.-L.L., and H.-N.D. provided reagents and suggestions; B.L., Y.R., X.S., B.Z., and Z.H. wrote the paper; and all the authors analyzed data.

ACKNOWLEDGMENTS

We would like to thank Drs. Hong-Bing Shu, Min Wu, and Lei Yin (Wuhan University); members of the Zhong lab and Huang lab; and the core facilities of the College of Life Sciences for technical help. This study was supported by grants from the Ministry of Science and Technology of China (2014CB542601 and 2013CB910700), National Natural Science Foundation of China (31371481, 31371427, 31521091, 81670140, 31671454, and 31622036), the Ministry of Education of China (20110141110016 and 201427), Wuhan University (2042017kf0199 and 2042017kf0242), State Key Laboratory of Veterinary Etiological Biology (SKLVEB2015KFKT001), and Program for New Century Excellent Talents in University (NCET) of Ministry of Education of China (NCET-12-0422). Y. Cheng is an employee of Wuhan Qlife Company. X.C. is a founder and shareholder of Wuhan Qlife Company.

Received: February 8, 2017
Revised: May 2, 2017
Accepted: June 22, 2017
Published: July 12, 2017

REFERENCES

Hayden, M.S., and Ghosh, S. (2008). Shared principles in NF-kappaB signaling. Cell *132*, 344–362.

Hayden, M.S., and Ghosh, S. (2012). NF-κB, the first quarter-century: remarkable progress and outstanding questions. Genes Dev. *26*, 203–234.

Hemmi, H., Takeuchi, O., Sato, S., Yamamoto, M., Kaisho, T., Sanjo, H., Kawai, T., Hoshino, K., Takeda, K., and Akira, S. (2004). The roles of two IkappaB kinase-related kinases in lipopolysaccharide and double stranded RNA signaling and viral infection. J. Exp. Med. *199*, 1641–1650.

Hinz, M., and Scheidereit, C. (2014). The IκB kinase complex in NF-κB regulation and beyond. EMBO Rep. *15*, 46–61.

Huang, J., Liu, T., Xu, L.G., Chen, D., Zhai, Z., and Shu, H.B. (2005). SIKE is an IKK epsilon/TBK1-associated suppressor of TLR3- and virus-triggered IRF-3 activation pathways. EMBO J. *24*, 4018–4028.

Ikushima, H., Negishi, H., and Taniguchi, T. (2013). The IRF family transcription factors at the interface of innate and adaptive immune responses. Cold Spring Harb. Symp. Quant. Biol. *78*, 105–116.

Ishikawa, H., and Barber, G.N. (2008). STING is an endoplasmic reticulum adaptor that facilitates innate immune signalling. Nature *455*, 674–678.

Kanarek, N., and Ben-Neriah, Y. (2012). Regulation of NF-κB by ubiquitination and degradation of the IκBs. Immunol. Rev. *246*, 77–94.

Kawai, T., Takahashi, K., Sato, S., Coban, C., Kumar, H., Kato, H., Ishii, K.J., Takeuchi, O., and Akira, S. (2005). IPS-1, an adaptor triggering RIG-I- and Mda5-mediated type I interferon induction. Nat. Immunol. *6*, 981–988.

Lei, C.Q., Zhong, B., Zhang, Y., Zhang, J., Wang, S., and Shu, H.B. (2010). Glycogen synthase kinase 3β regulates IRF3 transcription factor-mediated antiviral response via activation of the kinase TBK1. Immunity *33*, 878–889.

Li, S., Wang, L., Berman, M., Kong, Y.Y., and Dorf, M.E. (2011). Mapping a dynamic innate immunity protein interaction network regulating type I interferon production. Immunity *35*, 426–440.

Lin, D., Zhang, M., Zhang, M.X., Ren, Y., Jin, J., Zhao, Q., Pan, Z., Wu, M., Shu, H.B., Dong, C., and Zhong, B. (2015). Induction of USP25 by viral infection promotes innate antiviral responses by mediating the stabilization of TRAF3 and TRAF6. Proc. Natl. Acad. Sci. USA *112*, 11324–11329.

Liu, F., Xia, Y., Parker, A.S., and Verma, I.M. (2012). IKK biology. Immunol. Rev. *246*, 239–253.

Luo, W.W., Li, S., Li, C., Lian, H., Yang, Q., Zhong, B., and Shu, H.B. (2016). iRhom2 is essential for innate immunity to DNA viruses by mediating trafficking and stability of the adaptor STING. Nat. Immunol. *17*, 1057–1066.

Martinez-De Luna, R.I., Ku, R.Y., Lyou, Y., and Zuber, M.E. (2013). Maturin is a novel protein required for differentiation during primary neurogenesis. Dev. Biol. *384*, 26–40.

McWhirter, S.M., Fitzgerald, K.A., Rosains, J., Rowe, D.C., Golenbock, D.T., and Maniatis, T. (2004). IFN-regulatory factor 3-dependent gene expression is defective in Tbk1-deficient mouse embryonic fibroblasts. Proc. Natl. Acad. Sci. USA *101*, 233–238.

Pandey, S., Kawai, T., and Akira, S. (2014). Microbial sensing by Toll-like receptors and intracellular nucleic acid sensors. Cold Spring Harb. Perspect. Biol. *7*, a016246.

Perry, A.K., Chow, E.K., Goodnough, J.B., Yeh, W.C., and Cheng, G. (2004). Differential requirement for TANK-binding kinase-1 in type I interferon responses to toll-like receptor activation and viral infection. J. Exp. Med. *199*, 1651–1658.

Ren, Y., Zhao, Y., Lin, D., Xu, X., Zhu, Q., Yao, J., Shu, H.B., and Zhong, B. (2016). The type I interferon-IRF7 axis mediates transcriptional expression of Usp25 gene. J. Biol. Chem. *291*, 13206–13215.

Sakurai, H., Chiba, H., Miyoshi, H., Sugita, T., and Toriumi, W. (1999). IkappaB kinases phosphorylate NF-kappaB p65 subunit on serine 536 in the transactivation domain. J. Biol. Chem. *274*, 30353–30356.

Seth, R.B., Sun, L., Ea, C.K., and Chen, Z.J. (2005). Identification and characterization of MAVS, a mitochondrial antiviral signaling protein that activates NF-kappaB and IRF 3. Cell *122*, 669–682.

Shen, B., Zhang, J., Wu, H., Wang, J., Ma, K., Li, Z., Zhang, X., Zhang, P., and Huang, X. (2013). Generation of gene-modified mice via Cas9/RNA-mediated gene targeting. Cell Res. *23*, 720–723.

Song, G., Liu, B., Li, Z., Wu, H., Wang, P., Zhao, K., Jiang, G., Zhang, L., and Gao, C. (2016). E3 ubiquitin ligase RNF128 promotes innate antiviral immunity through K63-linked ubiquitination of TBK1. Nat. Immunol. *17*, 1342–1351.

Sun, X., Lu, B., Hu, B., Xiao, W., Li, W., and Huang, Z. (2014). Novel function of the chromosome 7 open reading frame 41 gene to promote leukemic megakaryocyte differentiation by modulating TPA-induced signaling. Blood Cancer J. *4*, e198.

Sun, H., Zhang, Q., Jing, Y.Y., Zhang, M., Wang, H.Y., Cai, Z., Liuyu, T., Zhang, Z.D., Xiong, T.C., Wu, Y., et al. (2017). USP13 negatively regulates antiviral responses by deubiquitinating STING. Nat. Commun. *8*, 15534.

Takeuchi, O., and Akira, S. (2010). Pattern recognition receptors and inflammation. Cell *140*, 805–820.

Wang, C., Chen, T., Zhang, J., Yang, M., Li, N., Xu, X., and Cao, X. (2009). The E3 ubiquitin ligase Nrdp1 'preferentially' promotes TLR-mediated production of type I interferon. Nat. Immunol. *10*, 744–752.

Wesche, H., Henzel, W.J., Shillinglaw, W., Li, S., and Cao, Z. (1997). MyD88: an adapter that recruits IRAK to the IL-1 receptor complex. Immunity *7*, 837–847.

Wu, J., and Chen, Z.J. (2014). Innate immune sensing and signaling of cytosolic nucleic acids. Annu. Rev. Immunol. *32*, 461–488.

Xu, L.G., Wang, Y.Y., Han, K.J., Li, L.Y., Zhai, Z., and Shu, H.B. (2005). VISA is an adapter protein required for virus-triggered IFN-beta signaling. Mol. Cell *19*, 727–740.

Yamamoto, M., Sato, S., Hemmi, H., Hoshino, K., Kaisho, T., Sanjo, H., Takeuchi, O., Sugiyama, M., Okabe, M., Takeda, K., and Akira, S. (2003). Role of adaptor TRIF in the MyD88-independent toll-like receptor signaling pathway. Science *301*, 640–643.

Yang, F., Tang, E., Guan, K., and Wang, C.Y. (2003). IKK beta plays an essential role in the phosphorylation of RelA/p65 on serine 536 induced by lipopolysaccharide. J. Immunol. *170*, 5630–5635.

Yao, J., and Qin, F. (2009). Interaction with phosphoinositides confers adaptation onto the TRPV1 pain receptor. PLoS Biol. *7*, e46.

Zhang, M., Zhang, M.X., Zhang, Q., Zhu, G.F., Yuan, L., Zhang, D.E., Zhu, Q., Yao, J., Shu, H.B., and Zhong, B. (2016). USP18 recruits USP20 to promote innate antiviral response through deubiquitinating STING/MITA. Cell Res. *26*, 1302–1319.

Zhang, Q., Lenardo, M.J., and Baltimore, D. (2017). 30 years of NF-κB: a blossoming of relevance to human pathobiology. Cell *168*, 37–57.

Zhong, B., Yang, Y., Li, S., Wang, Y.Y., Li, Y., Diao, F., Lei, C., He, X., Zhang, L., Tien, P., and Shu, H.B. (2008). The adaptor protein MITA links virus-sensing receptors to IRF3 transcription factor activation. Immunity *29*, 538–550.